ELSEVIER

Journal of Photochemistry and Photobiology A: Chemistry 106 (1997) 67–74

Journal of PHOTOCHEMISTRY AND PHOTOBIOLOGY A: CHEMISTRY

A study of substitution pathways in mononuclear ruthenium organometallic complexes by photochemistry

Nicholas E. Leadbeater

Centre for Inorganic Photochemistry, Department of Chemistry, Lensfield Road, Cambridge CB2 1EW, UK

Abstract

The photosubstitution reactions of d^8 metal carbonyls usually proceed with a high degree of stereospecificity. These studies aim to elucidate the mechanism of photosubstitution in $Ru(CO)_4(C_2H_4)$ and $Ru(CO)_4(PR_3)$ ($R \equiv Ph$, OMe) with CO, ethylene and tertiary phosphines. Research shows that photolysis induces the loss of a carbonyl group rather than an ethylene or phosphine ligand, the reaction taking place by a purely dissociative reaction pathway. In addition, the mechanisms of the thermal substitution reactions of $Ru(CO)_4(C_2H_4)$ with CO and tertiary phosphines are discussed. As a result of these investigations, a number of novel phosphine-containing mononuclear ruthenium complexes are reported. © 1997 Elsevier Science S.A.

Keywords: Mononuclear ruthenium organometallic complexes; Photochemistry; Substitution pathways

1. Introduction

Studies of unsaturated metal carbonyl compounds continue to be of fundamental interest due to their central role in both stoichiometric and catalytic reaction pathways [1]. Despite this, the molecular structures of many of the reactive intermediates formed in organometallic reactions are not fully understood. Results from this group and others have shown that photochemistry is an ideal technique for the generation of such intermediates, and, by vibrational analysis of the IR spectra, investigation of the reaction products and molecular orbital calculations, conjectures for the structures can be made. In this article, the photochemical syntheses of a number of known and novel mononuclear ruthenium fragments are reported and reaction mechanisms are suggested. Attention is focused on the photosubstitution of CO in $Ru(CO)_4(C_2H_4)$ (**1a**) and $Ru(CO)_4(PR_3)$ (**2a**) complexes by phosphines and ethylene. In addition, the thermal substitution chemistry of **1a** is discussed.

2. Results and discussion

*2.1. The synthesis, structure and substitution reactions of $Ru(CO)_4(C_2H_4)$ (**1a**)*

The η^2-olefin complex $Ru(CO)_4(C_2H_4)$ (**1a**) was first reported in 1974 as a product of the broad-band UV photolysis of a hydrocarbon solution of $Ru_3(CO)_{12}$ (**3**) in the presence of ethylene [2]. It was assigned a trigonal bipyramidal structure on the basis of IR analysis, the ethylene substituent occupying an equatorial site. This geometry is also predicted by frontier orbital calculations taking into account the nature of the bonding, the rotational barriers and the conformational preferences of the olefin [3,4]. In addition, it is calculated that the ethylene will prefer an orientation in the equatorial plane compared with a perpendicular position. Recent matrix isolation studies have confirmed this structural assignment [5]. It has been demonstrated in our group that both the rate of formation and the stability of the olefin complex can be increased greatly by performing the reaction at low temperatures using dichloromethane as a solvent instead of hydrocarbons such as hexane [6]

$$Ru_3(CO)_{12} \xrightarrow[\text{dichloromethane}]{h\nu,\ C_2H_4} Ru(CO)_4(C_2H_4)$$

The substitution reaction chemistry of **1a**, unlike the iron analogue **1b**, has been the subject of few studies [7,8]. However, it is suggested that the reaction of **1a** with a ligand L ($L \equiv PPh_3$, CO, pyridine) occurs via a dissociative pathway [9]

$$Ru(CO)_4(C_2H_4) \xrightarrow{-C_2H_4} [Ru(CO)_4] \xrightarrow{L} Ru(CO)_4L$$

This involves the formation of the highly reactive 16-electron complex $[Ru(CO)_4]$ (**4a**). The corresponding iron complex $[Fe(CO)_4]$ (**4b**) has been subject to a number of studies, and it has been concluded that the molecule has C_{2v}

PII S1010-6030(97)00041-5

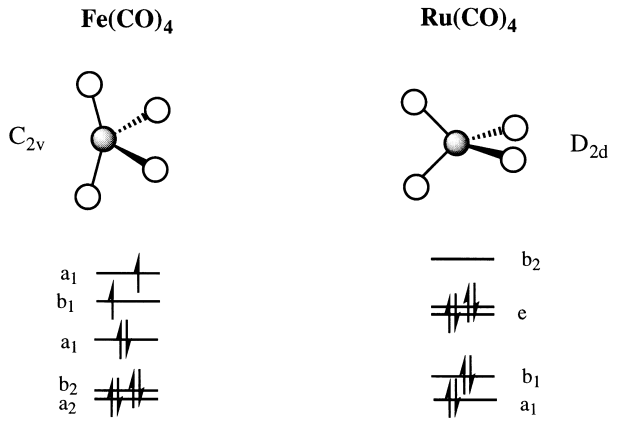

Fig. 1. The molecular structures and d orbital diagrams of $[Fe(CO)_4]$ and $[Ru(CO)_4]$.

geometry in the ground state [10–12]. Both of these observations and the fact that **4b** is paramagnetic point towards a triplet electronic ground state [13]. In contrast, it has been suggested that **4a** has a singlet electronic ground state [14]. By analogy with other d^8 low spin complexes, such as $[Ni(CN)_4]^{2-}$ and $[PtCl_4]^{2-}$, a square planar geometry is expected [15]. However, a plot of the orbital energy vs. the L–M–L angle shows that, for a strong π-acceptor ligand such as CO, the D_{4h} geometry is unstable with respect to D_{2d} distortion [11]. This is due to the rapid stabilization of the a_{1g} level of the square planar geometry gained on deformation to D_{2d} as a result of increased interaction with the π^* orbitals and decreased interaction with the σ antibonding orbitals of CO. A D_{2d} structure has indeed been proposed for **4a** on the basis of Hartree–Fock calculations [16]. Despite this, it is not possible to say with certainty that **4a** is generated in the singlet ground state, since heavy transition metals, such as ruthenium, can increase greatly the rate of triplet–singlet interconversion [17]. The molecular structures and d orbital diagrams for **4a** and **4b** are shown in Fig. 1 .

These results will form the basis for much of the following discussion. However, a cautionary note must be made. The structures of the reactive intermediates **4a** and **4b** proposed above are the result of gas phase and low temperature matrix studies. This paper is concerned primarily with reactions in solution. For this reason, it is necessary to assume that the intermediates are structurally analogous in all phases, but the role of the solvent in the reaction pathways must be taken into consideration.

An investigation of the electronic ground states of **4a** and **4b** allows an understanding to be reached of the observed differences in the rate of reaction of ligand substitution in **1a** and **1b**. Focusing our attention on the substitution of ethylene by carbon monoxide, results from this study and from coworkers show that the reaction occurs much more rapidly in the case of **1a** than **1b** [7]. This difference in reaction rate can be explained by the fact that both the dissociation of **1b** into **4b** and C_2H_4 and the reaction of **4b** with CO are spin forbidden in the ground state, whereas the corresponding processes for the ruthenium analogues **4a** and **1a** are spin allowed [12]. State correlation diagrams are shown in Fig. 2 and reaction pathways in Scheme 1, assuming that the principle of least motion is obeyed. [1]

The pathway for **4b** shown here involves spin changes to make the reaction spin and symmetry allowed, this being highly unfavourable. The fact that the reaction occurs at all may be a result of one of two possible processes. Firstly, there may be considerable spin–orbit coupling, making the reaction symmetry allowed as a result of an avoided crossing, probably with a low energy barrier (or at least substantially lower than that of the non-coupled reaction) [13]. Alternatively, lowering the symmetry of the metal carbonyl fragment and an eccentric approach of the incoming ligand, such as that shown in Scheme 2, may occur, resulting in the reaction being symmetry allowed, at least with respect to orbital symmetry [13].

[1] The principle of least motion states that the lowest activation energy for a reaction is that requiring the least motion of the nuclei and the least disruption of the original electronic distribution.

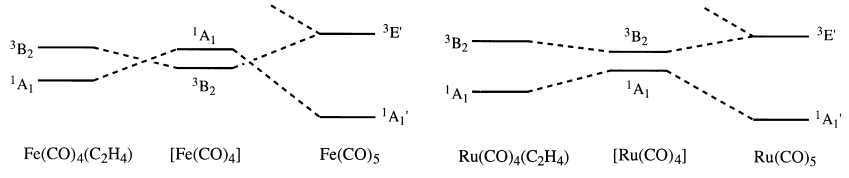

Fig. 2. State correlation diagrams for the reaction $M(CO)_4(C_2H_4) \xrightarrow{CO} M(CO)_5$.

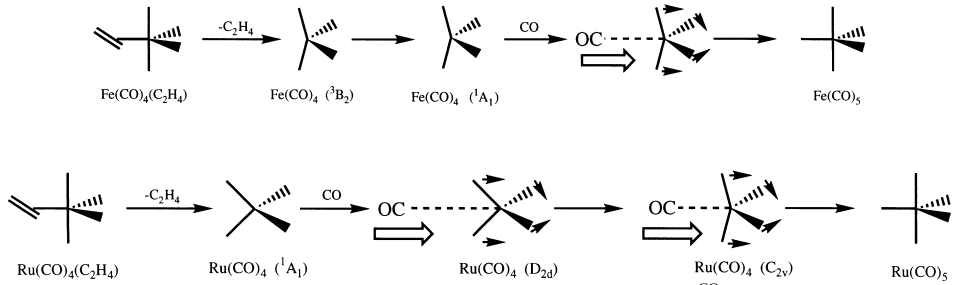

Scheme 1. Reaction pathways for the reaction $M(CO)_4(C_2H_4) \xrightarrow{CO} M(CO)_5$.

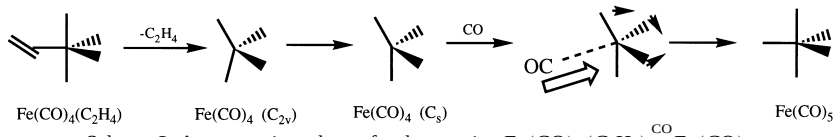

Scheme 2. An eccentric pathway for the reaction $Fe(CO)_4(C_2H_4) \xrightarrow{CO} Fe(CO)_5$.

Concerted path.

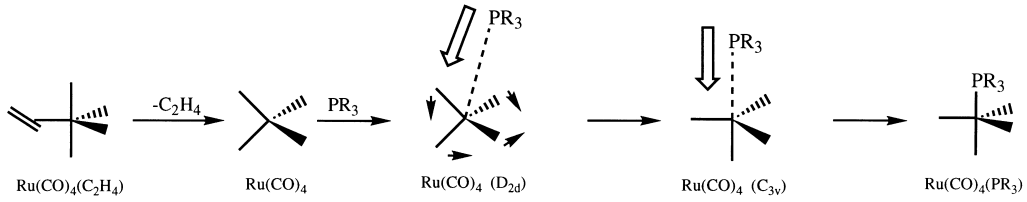

Non-concerted path.

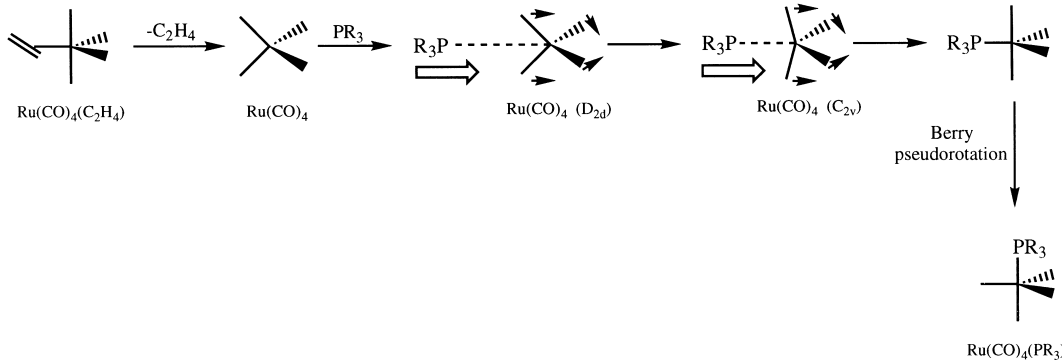

Scheme 3. Concerted and non-concerted reaction pathways for the substitution of the olefin in $Ru(CO)_4(C_2H_4)$ by a phosphine.

For the case of ruthenium, assuming that **4a** is a singlet, the reaction is spin allowed and proceeds along the least motion pathway. [2]

Since little attention has been focused on the substitution chemistry of **1a**, it is interesting to note that an S_N2 associative/dissociative mechanism is forbidden on orbital grounds. [3]

The addition of a tertiary phosphine, PR_3 ($R \equiv Ph, OMe$), to a solution of **1a** leads quantitatively to the monosubstituted product **2a**, vibrational analysis pointing towards an axial disposition of the phosphine ligand. The mechanism for this reaction is somewhat more complex than that for substitution of ethylene by CO, since the olefin is lost from an equatorial position and the incoming substituent must end up in an axial site. There are two possibilities: either a concerted process or the formation of an equatorially substituted isomer followed by Berry pseudo-rotation to form the observed structure [18]. Any concerted mechanism would involve the attack of the phosphine moiety along a highly unfavourable trajectory, as illustrated in Scheme 3. It is suggested that a non-concerted mechanism is most likely, the phosphine attacking along the A_1 reaction coordinate to form the C_{2v} equatorially substituted product. Driven by the increased bonding coefficient obtained from interaction with CO rather than PR_3 in the equatorial position, a rearrangement could then occur by a Berry pseudo-rotation mechanism to generate the most stable configuration. [4]

2.2. Photosubstitution in $Ru(CO)_4(C_2H_4)$ (**1a**)

Broad-band UV photolysis of a dichloromethane solution of **1a** under an atmosphere of ethylene leads quantitatively to the known bis-substituted complex $Ru(CO)_3(C_2H_4)_2$ (**5a**) [19]. This is believed to occur by a dissociative mechanism, the photochemical labilization of a CO group occurring before reaction with the ethylene.

$$Ru(CO)_3\{P(OMe)_3\}(C_2H_4) \xrightarrow{Ph_2P(CH_2)_2PPh_2} Ru(CO)_3\{P(OMe)_3\}\{Ph_2P(CH_2)_2PPh_2\}$$

This involves the formation of the reactive intermediate $[Ru(CO)_3(C_2H_4)]$ (**6a**). This photoproduct has been observed in 3-methylpentane glasses at 55 K, but little comment has been made [19]. It is the aim of this section to investigate the geometry and reactivity of this intermediate.

[2] Having said this, it would not be unreasonable for triplet **4a** to react more rapidly than triplet **4b** due to the increased spin–orbit coupling found in heavier transition metals. This, however, is unlikely to be the case.

[3] It is assumed that the ligand orbitals are unperturbed during the course of the reaction and that C_{2v} symmetry is maintained throughout the associative step.

[4] The exact mechanism will be highly dependent on the trans basal angle in the $[Ru(CO)_4]$ fragment.

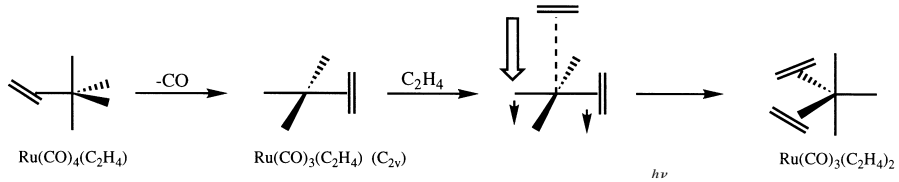

Scheme 4. A least motor pathway for the reaction $Ru(CO)_4(C_2H_4) \xrightarrow[C_2H_4]{h\nu} Ru(CO)_3(C_2H_4)_2$.

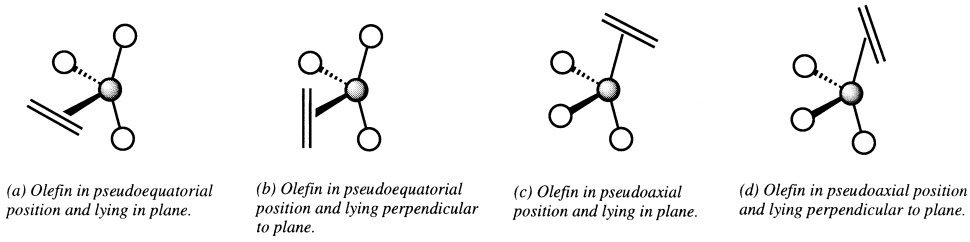

Fig. 3. Possible molecular arrangements of $[Fe(CO)_3(C_2H_4)]$ in C_s symmetry.

Since the $^1A_1$ singlet state of **4a** is significantly more stable than the $^3B_2$ state and substitution of an olefin for CO in **6a** will not alter significantly the extent of π backbonding in the system and hence the ligand field, it may be proposed that **6a** also has a singlet electronic ground state [20].

By analogy with the argument forwarded for the structure of **4a**, a square planar geometry may be assigned to **6a** at first glance. Such a geometry is well known for the isoelectronic complex $[PtCl_3(C_2H_4)]^-$, the olefin lying perpendicular to the plane [21]. Attack by the second olefin could then be envisaged from either the top or bottom of the molecule, the bound ethylene and the CO trans to it defining the equatorial plane of the bis-substituted product. This is shown in Scheme 4.

Despite this being the expected pathway, it is necessary to be cautious in saying that this is indeed the mechanism involved. As shown for **4a**, distortion from the idealized square planar geometry may occur. This is in contrast with the isoelectronic complex $[PtCl_4]^{2-}$ which maintains D_{4h} symmetry. The difference may be explained by the difference in π donor/acceptor character of the CO vs. the Cl ligand, the deformation of $[PtCl_4]^{2-}$ not being concomitant with a decrease in energy of the a_1 orbital [22].

As a result, it is not unreasonable to predict that **6a** will distort from the archetypal square planar geometry resulting in a C_s structure, as has been demonstrated for $[Fe(CO)_3(C_2H_4)]$ (**6b**) [20]. There are four possible molecular configurations. The olefin may lie in a pseudo-equatorial site, either lying in the plane or perpendicular to it, or in a pseudo-axial site, again either in the plane or perpendicular to it [20]. These possibilities are illustrated in Fig. 3.

The employment of Fenske–Hall calculations to assess the bonding in **6b** show the most stable structure to be that with the olefin in a pseudo-equatorial position and lying in the equatorial plane [20]. Although these calculations are insensitive to the spin multiplicity, they are affected by the orbital energy. As a result of the difference in orbital energy, and hence geometry, between **3a** and **3b**, it follows that it is not possible to infer identical structures for **6a** and **6b**. Instead, it is suggested that **6a** has a structure based on the D_{2d} geometry of **3a** with a carbonyl replaced by the ethylene moiety (reducing the symmetry of the molecule to C_s). This is subtly different from the case of **6b** which is based on the C_{2v} geometry of **3b**. [5] The proposed structures for **6a** and **6b** are shown in Fig. 4. It is possible to envisage the attack of ethylene on the less hindered side of **6a** forming the product **5a** and restoring the C_{2v} symmetry (Scheme 5).

$Fe(CO)_3(C_2H_4)$ **$Ru(CO)_3(C_2H_4)$**

Fig. 4. The proposed structures of $[Fe(CO)_3(C_2H_4)]$ in C_s symmetry.

2.3. Photosubstitution in $Ru(CO)_4(PR_3)$ (2a)

Broad-band UV irradiation of a solution of **2a** in the presence of excess phosphine (PR_3) leads to the generation of the bis-substituted product $Ru(CO)_3(PR_3)_2$ (**7a**), vibrational analysis pointing towards a di-axial disposition of the phosphine ligands [23]. Again it is postulated that the reaction occurs by a dissociative mechanism, and observations point to photolabilization of the axial carbonyl group rather than, as may have been expected, an equatorial CO [23]. This leads to an interesting discussion of the structure of the $[Ru(CO)_3(PR_3)]$ (**8a**) intermediate involved. Photolabilization of the axial CO ligand leads initially to the formation of **8a** in a C_{3v} geometry, this being observed for the intermediate in low temperature organic glasses [23]. The prin-

[5] The difference in geometry between the iron and ruthenium analogues **6a** and **6b** will again be dependent on the trans basal angle of the D_{2d} structure.

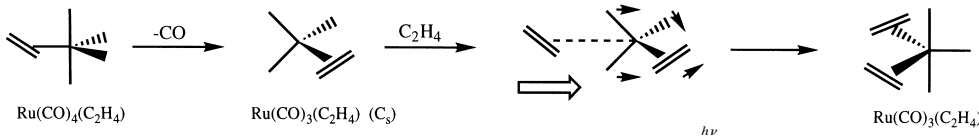

Scheme 5. An alternative pathway for the reaction $Ru(CO)_4(C_2H_4) \xrightarrow[C_2H_4]{h\nu} Ru(CO)_3(C_2H_4)_2$.

ciple of least motion would point towards the second phosphine ligand attacking at the least hindered side of the molecule, forming the D_{3h} product without the need for further molecular rearrangement (mechanism 1). Alternatively, the C_{3v} fragment could distort to a C_s structure, although this may not differ greatly from the C_{3v} geometry. It would be expected that the phosphine would maintain a pseudo-axial site. Attack on **8a** by free phosphine along the C_s pathway would lead to either the bis-axial-equatorial or di-equatorial isomer of the product (mechanisms 2 and 3) depending on which side the incoming phosphine attacks. Rearrangement by a Berry pseudo-rotation mechanism could then occur, this being driven by the increased stability of three equatorially disposed carbonyl groups rather than two in the product and the increase in symmetry on rearrangement. These mechanisms are shown in Scheme 6.

It is concluded that, certainly at low temperatures, mechanism 1 is favoured on the grounds that it both obeys the principle of least motion and is less sterically and energetically demanding. Although an identical mechanism may be inferred for room temperature substitution, calculations of the relative energies of the C_{3v} and C_s geometries of **8a** are needed before any definitive argument may be forwarded. It may well be that the potential energy surface between the two geometries is soft, leading to an interesting study of the temperature effects on the reaction mechanism.

It is clear that the arrangement of the ligand groups in the phosphine-substituted ruthenium carbonyl complexes is

Mechanism 1.

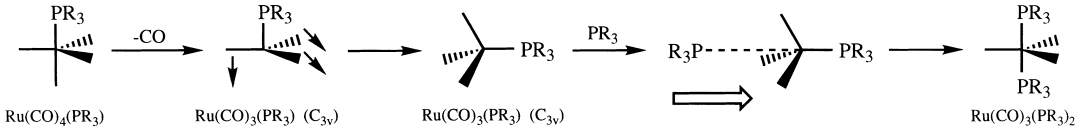

Mechanism 2.

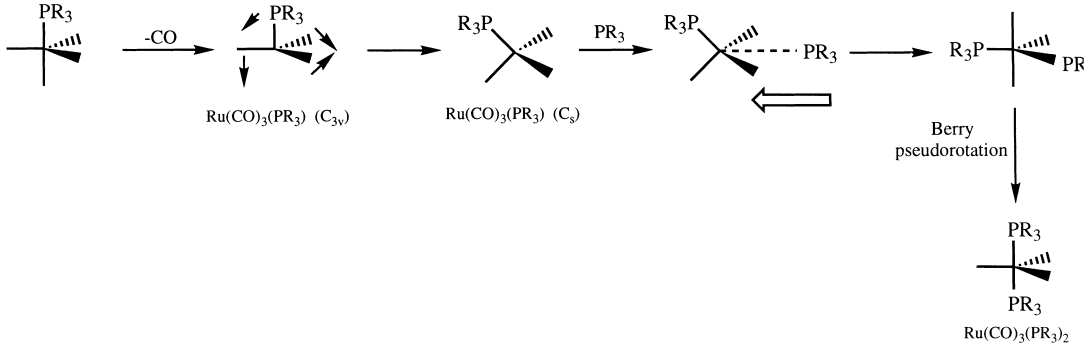

Mechanism 3.

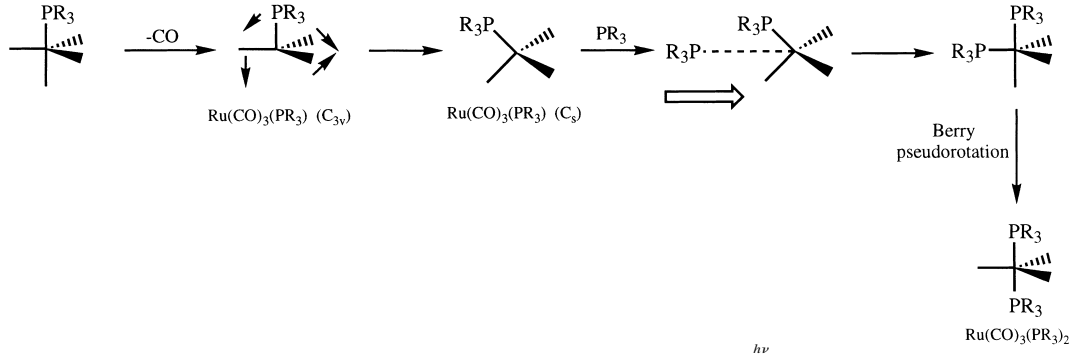

Scheme 6. Possible reaction pathways for the reaction $Ru(CO)_4(PR_3) \xrightarrow[PR_3]{h\nu} Ru(CO)_3(PR_3)_2$.

determined not by the steric bulk of the ligands, but by the extent of orbital overlap and the degree of symmetry attained. Steric control of the reaction pathway would result in the formation of the bis-equatorial isomer of the product, but this is not the case, maximum stability being achieved with the bulky phosphine groups occupying the axial positions in the D_{3h} structure.

We report here the preliminary findings of research into the photochemistry of **2a** in the presence of ethylene.

It is well known that neutral mononuclear ruthenium complexes, such as $Ru(CO)_4(PPh_3)$ and $Ru(CO)_3(PPh_3)_2$, are catalyst precursors for the photochemical carbonylation of benzene, the hydrogenation and isomerization of olefinic substrates, the hydroformylation of ethylene and propylene and the hydrogenation of benzaldehyde to benzoic acid [24,25]. It is suggested that the principal catalyst precursor in all these cases is the monophosphine complex, other starting materials being converted into this before entering the catalytic cycle. The key photochemical step is proposed to be CO dissociation, generating $[Ru(CO)_3(PPh_3)]$, this then either coordinating an olefinic bond or backreacting with CO to regenerate $Ru(CO)_4(PPh_3)$. As a result, the study of the reactivity of $[Ru(CO)_3(PPh_3)]$ with olefins is of key importance in understanding more fully the catalytic cycles involved in these processes and the nature of the reactive intermediates intimately involved.

Broad-band UV photolysis of a dichloromethane solution of **2a** under an atmosphere of ethylene leads to a single product, the vibrational analysis of which suggests the axial-equatorial disubstituted complex $Ru(CO)_3(PR_3)(C_2H_4)$ (**9a**)

$$Ru(CO)_4(PPh_3) \xrightarrow[C_2H_4]{h\nu} Ru(CO)_3(PPh_3)(C_2H_4)$$

This class of compound, prepared in our room temperature studies, will prove of value for the fulfilment of these aims.

Assuming that **8a** is formed in the C_{3v} geometry discussed above, the direct formation of the desired isomer of the phosphine–olefin product would be unlikely. Instead, it is proposed that either distortion of **8a** occurs to yield a C_s geometry, followed by attack of the olefin (mechanisms 1 and 2), or alternatively, the olefin attacks the C_{3v} fragment to yield the di-axial isomer of the product which then rearranges to the axial-equatorial congener driven by the increased stability of the olefin in an equatorial position (mechanism 3). These mechanisms are shown in Scheme 7.

Although mechanism 1 yields the observed isomer of the product without the need for rearrangement, attack of the olefin must occur on the sterically more crowded side of the molecule. This will be less favoured compared with attack on the less hindered side of the C_s intermediate (mechanism 2), but the latter requires subsequent rearrangement to yield the observed isomer of **9a**.

On balance, mechanism 3 is most likely at low temperature on the basis of both orbital and steric considerations. Again it is difficult to determine which of the mechanisms is most appropriate at room temperature without the calculation of both the geometry of **8a** and the R_3P–Ru–CO and OC–Ru–CO bond angles. [6]

The reaction of a tertiary phosphine PR'_3 ($R' \equiv$ Ph and OMe) with **9a** results in the formation of the bis-phosphine product $Ru(CO)_3(PR_3)(PR'_3)$ (**10a**) in quantitative yield

$$Ru(CO)_3(PR_3)(C_2H_4) \xrightarrow{PR'_3} Ru(CO)_3(PPh_3)(PR'_3)$$

The lack of dependence of the reaction rate on the ligand concentration points towards the expected dissociative mechanism. It is interesting to note, however, that the rate of substitution in **9a** is considerably slower than in the case of **1a**, this being explained by the increased backbonding from the metal to the olefin in **9a** compared with **1a**. The mechanism for this reaction is of interest since, unlike the case of **2a**, a ligand is removed from an equatorial site initially producing a C_s fragment which may subsequently rearrange to a C_{3v} geometry.

Reaction of $Ru(CO)_3\{P(OMe)_3\}(C_2H_4)$ with 1,2-bis-(diphenylphosphino)ethane results in the formation of the novel mononuclear complex $Ru(CO)_3\{P(OMe)_3\}$-$\{\eta^1$-$Ph_2P(CH_2)_2PPh_2\}$ (**11a**), the phosphine substituents occupying the axial sites

$$Ru(CO)_3\{P(OMe)_3\}(C_2H_4) \xrightarrow{Ph_2P(CH_2)_2PPh_2} Ru(CO)_3\{P(OMe)_3\}\{Ph_2P(CH_2)_2PPh_2\}$$

This compound is considerably more stable than the reported $Ru(CO)_4\{\eta^1$-$Ph_2P(CH_2)_2PPh_2\}$ complex which has a limited lifetime in solution before trimerizing to a number of mononuclear and cluster complexes of which the main products are $Ru(CO)_3\{Ph_2P(CH_2)_2PPh_2\}$, $Ru_3(CO)_{12}$ and $Ru_3(CO)_{10}\{Ph_2P(CH_2)_2PPh_2\}$ [26,27]. The increased stability of **12** implies that the activation energy for the trimerization and chelation processes is increased by introducing trimethylphosphite into the complex, this being attributed to the strong σ donor interaction of the phosphite strengthening the remaining Ru–CO bonds.

3. Conclusions

The applicability of photochemistry to the synthesis of key organometallic intermediates has been highlighted and, from the results of our group and others, proposals for a number of reaction mechanisms have been discussed.

As more is learnt about the reaction intermediates, it becomes clearer that closely related reactions need not necessarily have the same mechanism. In addition, it has been shown that the geometry of the reactive intermediates is of key importance in governing the rate of reaction and the stereochemistry of the products formed.

[6] The geometry determining whether mechanism 3 is favoured over mechanisms 1 and 2; the bond angles determining by how much the energies of mechanisms 1 and 2 differ.

Mechanism 1.

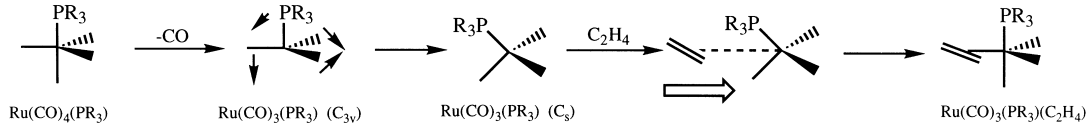

Mechanism 2.

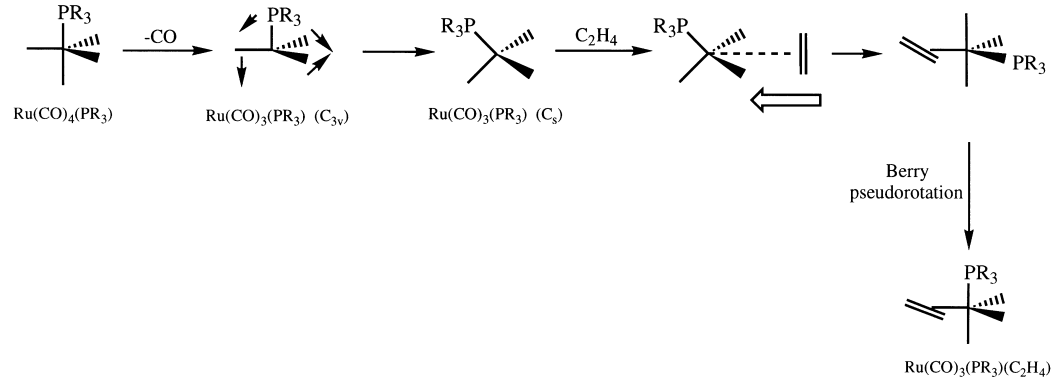

Mechanism 3.

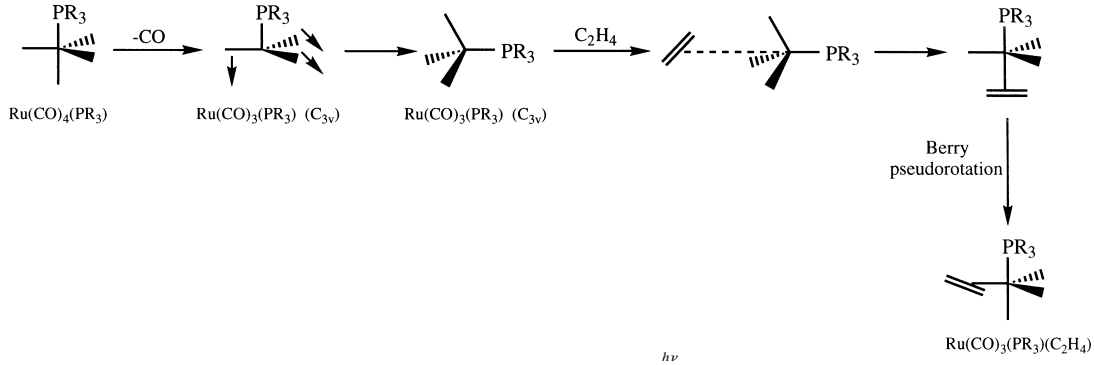

Scheme 7. Pathways for the reaction $Ru(CO)_4(PPh_3) \xrightarrow[C_2H_4]{h\nu} Ru(CO)_3(PPh_3)(C_2H_4)$.

4. Experimental details

4.1. General experimental

All manipulations were carried out using dry nitrogen via standard techniques. All solvents were dried and freshly distilled under nitrogen prior to use.

All photochemical reactions were performed in a specially designed glass reaction vessel fitted with a gas bubbler, reflux condenser and cooling finger. A 125 W medium pressure mercury lamp was used as the irradiation source. IR spectra were recorded using a Perkin–Elmer 1710 Fourier transform IR spectrometer. NMR spectra were recorded using a Bruker WP250 Fourier transform NMR spectrometer and data are reported in units of parts per million relative to a standard. In the case of ^{31}P NMR spectra, all chemical shifts are relative to $P(OMe)_3$ and, for ^{1}H NMR spectra, the solvent resonance was used as an internal standard.

Literature methods were used to prepare the starting material $Ru_3(CO)_{12}$ [28].

4.2. Photochemical generation of $Ru(CO)_4(C_2H_4)$ in dichloromethane [2]

A dichloromethane solution of $Ru_3(CO)_{12}$ (100 mg) was irradiated and a flow of ethylene was maintained throughout the photolysis. The solution was maintained below 0 °C by means of a cooling finger. The solution became colourless after approximately 1 h, indicating the presence of the mononuclear species. Yield: quantitative by IR. IR ν_{CO} (CH_2Cl_2) (cm^{-1}): 2105 (m), 2023 (vs), 1987 (s).

4.3. Reaction of $Ru(CO)_4(C_2H_4)$ with tertiary phosphines PR_3 ($R \equiv Ph$, OMe)

An excess of phosphine was added to a solution of $Ru(CO)_4(C_2H_4)$ in dichloromethane and the mixture

was stirred for 1 h at 0 °C. A quantitative yield by IR of the phosphine-substituted product $Ru(CO)_4(PR_3)$ was obtained. IR ν_{CO} (CH_2Cl_2) (cm^{-1}): $Ru(CO)_4(PPh_3)$: 2056 (s), 1986 (m), 1952 (vs); $Ru(CO)_4\{P(OMe)_3\}$: 2063 (m), 1944 (vs, br).

4.4. Photochemical generation of $Ru(CO)_3(C_2H_4)_2$ in dichloromethane [19]

Irradiation of a dichloromethane solution of $Ru(CO)_4(C_2H_4)$ under an atmosphere of ethylene leads, within 1 h, to a quantitative yield by IR of the bis-olefin complex $Ru(CO)_3(C_2H_4)_2$. IR ν_{CO} (CH_2Cl_2) (cm^{-1}): 2079 (w), 2002 (m), 1992 (vs).

4.5. Photolysis of $Ru(CO)_4(PPh_3)$ with excess triphenylphosphine [23]

Irradiation of a dichloromethane solution of $Ru(CO)_4(PPh_3)$ in the presence of a threefold excess of triphenylphosphine leads, within 1 h, to a quantitative yield by IR of the bis-substituted complex $Ru(CO)_3(PPh_3)_2$. IR ν_{CO} (CH_2Cl_2) (cm^{-1}): 1895.

4.6. Photolysis of an ethylene-saturated solution of $Ru(CO)_4(PR_3)$ ($R \equiv Ph$, OMe)

Irradiation of an ethylene-purged dichloromethane solution of $Ru(CO)_4(PR_3)$ leads, within 2 h, to a colourless product showing three peaks in the ν_{CO} region of the IR spectrum. Vibrational analysis indicates the formation of the phosphine–olefin complex $Ru(CO)_3(PR_3)(C_2H_4)$. Yield: 85% by IR. IR ν_{CO} (CH_2Cl_2) (cm^{-1}): $Ru(CO)_3(PPh_3)(C_2H_4)$: 2018 (m), 1944 (s), 1916 (vs); $Ru(CO)_3\{P(OMe)_3\}(C_2H_4)$: 2029 (m), 1956 (s), 1923 (vs).

4.7. Reaction of $Ru(CO)_3(PR_3)(C_2H_4)$ ($R \equiv Ph$, OMe) with PR'_3 ($R' \equiv Ph$, OMe)

Addition of excess phosphine to a dichloromethane solution of $Ru(CO)_3(PPh_3)(C_2H_4)$ leads, within 3 h, to the corresponding bis-substituted product $Ru(CO)_3(PR_3)(PR'_3)$ as characterized by IR. Yield: quantitative by IR. IR ν_{CO} (CH_2Cl_2) (cm^{-1}): $Ru(CO)_3(PPh_3)\{P(OMe)_3\}$: 1905 (vs), 1898 (s, sh); $Ru(CO)_3\{P(OMe)_3\}_2$: 1932 (vs), 1921 (vs). ^{31}P NMR (ppm): $Ru(CO)_3(PPh_3)\{P(OMe)_3\}$: -101.5(s), -104.4(s).

4.8. Reaction of $Ru(CO)_3\{P(OMe)_3\}(C_2H_4)$ with 1,2-bis-(diphenylphosphino)ethane (dppe)

The addition of an equivalent of dppe to a solution of $Ru(CO)_3\{P(OMe)_3\}(C_2H_4)$ results in the formation of a colourless product within 2 h. Vibrational analysis indicates the formation of the novel mononuclear complex $Ru(CO)_3\{P(OMe)_3\}\{\mu^1\text{-}Ph_2P(CH_2)_2PPh_2\}$. Yield: 80% by IR. IR ν_{CO} (CH_2Cl_2) (cm^{-1}): 1948 (vs), 1900 (m, br). ^{31}P NMR: -101.9 (s), -103.9 (s), -131.3 (s).

Acknowledgements

I thank the EPSRC and Magdalene College, Cambridge, for financial support. I am grateful to all coworkers, particularly A.J. Edwards and G.P. Shields. I am especially grateful to Professor Lord Lewis and Dr P.R. Raithby for all of their guidance and advice.

References

[1] P.C. Ford, Acc. Chem. Res. 14 (1981) 31. R.M. Laine, J. Mol. Catal. 14 (1982) 137. J.-M. Basset, A.K. Smith, J. Mol. Catal. 2 (1977) 229. R. Ugo, R. Psaro, J. Mol. Catal. 20 (1983) 53. R. Whyman, Philos. Trans. R. Soc. London, A 308 (1982) 131.
[2] B.F.G. Johnson, J. Lewis, M.V. Twigg, J. Organomet. Chem. 67 (1974) C75.
[3] T.A. Albright, R. Hoffmann, J.C. Thibeault, D.L. Thorn, J. Am. Chem. Soc. 101 (1979) 6850.
[4] R. Hoffmann, A.R. Rossi, Inorg. Chem. 14 (1975) 365.
[5] F.-W. Grevels, J.G.A. Reuvers, J. Takats, J. Am. Chem. Soc. 103 (1981) 4069.
[6] A.J. Edwards, N.E. Leadbeater, P.R. Raithby, J. Lewis, J. Organomet. Chem. 503 (1995) 15.
[7] G. Cardiaci, Inorg. Chem. 13 (1974) 368.
[8] For the substitution chemistry of $Fe(CO)_4(C_2H_4)$, see: G. Cardiaci, Inorg. Chem. 13 (1974) 2974; P.M. Burkinshaw, D.T. Dixon, J.A.S. Howell, J. Chem. Soc., Dalton Trans. (1980) 999; A.Z. Rubezhov, S.P. Gubin, Adv. Organomet. Chem. 10 (1972) 347; F.U. Axe, D.S. Marynick, J. Am. Chem. Soc. 106 (1984) 6230.
[9] R. Huq, A.J. Poë, S. Chawla, Inorg. Chim. Acta 38 (1980) 121.
[10] M. Poliakoff, J.J. Turner, J. Chem. Soc., Dalton Trans. (1973) 1351. M. Poliakoff, J.J. Turner, J. Chem. Soc., Dalton Trans. (1974) 2276. J.K. Burdett, Inorg. Chem. 14 (1975) 375. A.J. Ouderkirk, E. Weitz, J. Chem. Phys. 79 (1983) 1089.
[11] J.K. Burdett, J. Chem. Soc., Faraday Trans. 2 70 (1974) 1599.
[12] M. Poliakoff, E. Weitz, Acc. Chem. Res. 20 (1987) 408.
[13] C. Daniel, M. Bénard, A. Dedieu, R. Weist, A. Veillard, J. Phys. Chem. 88 (1984) 4805.
[14] T. Zeigler, V. Tschinke, C. Ursenbach, J. Am. Chem. Soc. 109 (1987) 4825. T. Zeigler, V. Tschinke, L. Fan, A. Becke, J. Am. Chem. Soc. 111 (1989) 9177. P.L. Bogdan, E. Weitz, J. Am. Chem. Soc. 111 (1989) 3163. A.W. Ehlers, G. Frenking, Organometallics 14 (1995) 423.
[15] R.G. Hazell, S.E. Rasmussen, Acta Chem. Scand. 23 (1969) 61. R.G. Dickinson, J. Am. Chem. Soc. 44 (1922) 2404.
[16] T. Zeigler, Inorg. Chem. 25 (1986) 2721.
[17] J.I. Steinfeld, Molecules and Radiation, Harper and Row, 1974.
[18] R.S. Berry, J. Chem. Phys. 32 (1960) 933.
[19] Y.-M. Wuu, J.G. Bentsen, C.G. Brinkley, M.S. Wrighton, Inorg. Chem. 26 (1987) 530.
[20] T.M. Barnhart, R.F. Fenske, R.J. McMahon, Inorg. Chem. 31 (1992) 2679.
[21] J.A.J. Jarvis, B.T. Kilbourn, P.G. Owston, Acta Crystallogr. Sect. B 27 (1971) 366.
[22] M. Elian, R. Hoffmann, Inorg. Chem. 14 (1975) 1058.
[23] D.K. Liu, C.G. Brinkley, M.S. Wrighton, Organometallics 3 (1984) 1450.
[24] J.L. Graff, R.D. Sanner, M.S. Wrighton, Organometallics 1 (1982) 837.
[25] E.M. Gordon, R. Eisenberg, J. Mol. Catal. 45 (1988) 57.
[26] A.J. Edwards, N.E. Leadbeater, J. Lewis, P.R. Raithby, J. Organomet. Chem., in press.
[27] G.-Y. Kiel, J. Takats, Organometallics 8 (1989) 839.
[28] B.F.G. Johnson, J. Lewis, Inorg. Synth. 13 (1972) 92.